

**Zeitschrift:** Helvetica Physica Acta  
**Band:** 58 (1985)  
**Heft:** 2-3

**Artikel:** On the structural classification of double-octet AB<sub>2</sub> compounds  
**Autor:** Andreoni, Wanda  
**DOI:** <https://doi.org/10.5169/seals-115592>

### **Nutzungsbedingungen**

Die ETH-Bibliothek ist die Anbieterin der digitalisierten Zeitschriften auf E-Periodica. Sie besitzt keine Urheberrechte an den Zeitschriften und ist nicht verantwortlich für deren Inhalte. Die Rechte liegen in der Regel bei den Herausgebern beziehungsweise den externen Rechteinhabern. Das Veröffentlichen von Bildern in Print- und Online-Publikationen sowie auf Social Media-Kanälen oder Webseiten ist nur mit vorheriger Genehmigung der Rechteinhaber erlaubt. [Mehr erfahren](#)

### **Conditions d'utilisation**

L'ETH Library est le fournisseur des revues numérisées. Elle ne détient aucun droit d'auteur sur les revues et n'est pas responsable de leur contenu. En règle générale, les droits sont détenus par les éditeurs ou les détenteurs de droits externes. La reproduction d'images dans des publications imprimées ou en ligne ainsi que sur des canaux de médias sociaux ou des sites web n'est autorisée qu'avec l'accord préalable des détenteurs des droits. [En savoir plus](#)

### **Terms of use**

The ETH Library is the provider of the digitised journals. It does not own any copyrights to the journals and is not responsible for their content. The rights usually lie with the publishers or the external rights holders. Publishing images in print and online publications, as well as on social media channels or websites, is only permitted with the prior consent of the rights holders. [Find out more](#)

**Download PDF:** 16.09.2025

**ETH-Bibliothek Zürich, E-Periodica, <https://www.e-periodica.ch>**

# On the structural classification of double-octect $AB_2$ compounds

By Wanda Andreoni, Institut de Physique Expérimentale,  
Ecole Polytechnique Fédérale de Lausanne, CH-1015  
Lausanne, Switzerland

(27. VII. 1984)

In honor of Emanuel Mooser's 60th birthday

*Abstract.* Nodal radii, i.e. the outermost nodes of valence atomic wavefunctions, are introduced as basic elements in the coordinates of structural maps of solids. Application to double-octect compounds of non-transition elements successfully separates out the different structures, in particular '3-dimensional' packings from layer configurations, and arrangements with different coordination numbers (from 2 to 9). Some difficulty is found only for mercury dihalides. Pressure and temperature induced structural transformations are also discussed. Configurations of molecules are also classified within the same scheme.

## 1. Introduction and definition of structural coordinates

One of the most fascinating questions of solid state physics is to explain the structure that a given compound adopts at given pressure and temperature. Recently, total electron energy calculations have become feasible from first principles [1] and equilibrium structures at  $T = 0$  have sometimes been predicted successfully for elemental crystals [2] as well as for binary octect compounds [3]. However, so far, such calculations have failed to provide an understanding of the physical factors which determine one specific configuration as the equilibrium structure. A different approach to this problem is based on molecular dynamics calculations, which have allowed recently to predict successfully the whole ( $p, T$ ) diagram of AgI [4] and the  $NaCl \rightarrow CsCl$  transformation of KCl under pressure [5]. Here, a scheme for the interatomic interactions is chosen on a semi-empirical basis and contains ad hoc parameters which do not permit a direct interpretation.

An alternative (or rather a complement) to the above methods, which dates back to the early days of solid state physics [6], is the construction of bidimensional plots (structural maps) for given families of compounds. Two coordinates characterize each compound and the plot is deemed successful if the graph points turn out to assume a cluster configuration, with different domains representing different structures. The art of constructing these maps lies in the choice of the two coordinates. Here, the framework is always semiempirical but can in principle be much easier to follow and to interpret, since there are only two parameters.

The origin of modern structural classifications of this type is the Mooser-Pearson plot [7] of octect AB compounds. The new feature of the Mooser-Pearson work was the introduction of quantum mechanical concepts into the empirical scheme, through the use of an effective quantum number  $\bar{n}$  as one of

the coordinates. From that time (1959) on, solid state physics has witnessed the flourishing of structural maps which use fully quantum-mechanical elements but are still empirical in the construction of the coordinates, e.g. Phillips–Van Vechten plot [8] of octect AB compounds, Miedema's classification [9] of metal alloys and a number of maps of binary compounds based on orbital pseudopotential radii [10]. [For comprehensive reviews see Ref. 11].

Here, we concentrate on the structural maps based on orbital radii. We feel that, in spite of the undoubted success of pseudopotential-radii-based structural maps for AB compounds [12], a big effort must still be made before we can gain a true understanding of the reasons why they work so well. We shall not attempt to solve this problem here. We think that a systematic attack on a number of different classes of compounds may be useful, especially if it reveals both successes and failures of a given plot. Attempts made recently by Burdett et al. [10, 13] on  $AB_2$  and  $AB_2C_3$ -spinel compounds claim a success which is only in part reproducible. We shall discuss this point for the  $AB_2$  compounds (Section III).

We shall focus on  $AB_2$  double-octects of non-transition elements for which we present a new structural map. Our scheme, which is also semi-empirical, makes use of the *nodal radii* [14, 15]  $\mathcal{N}_l$  (i.e. the outermost nodes of the atomic valence electrons wavefunctions) as atomic orbital parameters. This choice is in our opinion more *fundamental* than that of the turning points  $S_l$  of non-local pseudopotentials (pseudopotential radii) since the latter depend strongly on the specific form of the pseudopotential chosen (cf. Zunger's radii and Simons–Bloch radii).

The special properties of nodal radii are discussed in a separate paper [15], in particular: i) their transferability from the isolated atom to the atomic aggregates and ii) the independence of their values, to a large extent, from the approximation used in the all-electron atomic calculations, i.e. local-density approximation of the density functional theory [16], Hartree–Fock approximation [17] or the Hartree–Fock–Slater simplified version [18].

These two properties (i) and ii)) allow us to use here nodal radii  $\mathcal{N}_l$  as basic elements for a structural map of solids. In analogy with previous works, the coordinates of our plot are linear combinations of *s* and *p*-radii ( $\mathcal{N}_0$  and  $\mathcal{N}_1$ ). For each element *E* we define two characterizing quantities:

$$\begin{aligned} y_E &= \left( \frac{1}{1+w} \right) (\mathcal{N}_0 + w\mathcal{N}_1) \\ x_E &= \left( \frac{1}{1+w} \right) (w\mathcal{N}_0 - \mathcal{N}_1) \end{aligned} \tag{1a}$$

and for each  $AB_2$  compound we define two coordinates:

$$\begin{aligned} Y(AB_2) &= y_B - y_A \\ X(AB_2) &= x_A + x_B \end{aligned} \tag{1b}$$

The only parameter, *w*, is chosen in an empirical way. The values we use here for the  $\mathcal{N}_l$ 's are taken from Hartree–Fock wavefunctions. For Pb and Hg, we use the results of Dirac–Hartree–Fock–Slater calculations [19].

In Section II, we shall briefly describe the different structures of the  $AB_2$  double-octect compounds, which present an interesting variety. We will present our structural plot and discuss it in some detail. In particular, we will point out the position of glassy materials and of superionic conductors in the map. One of our coordinates will be shown to correlate with the conformation of dihalide molecules. We will point out the failure of these coordinates to describe well compounds of multivalent ions like Pb, i.e. to predict the correct structure of lead dihalides and dichalcogenides at the same time. We will try to understand the reason for this.

In Section III, we will briefly discuss a previous plot by Burdett et al. [10, 13] and compare their findings with ours.

## II. Description of the structures and nodal-radii-based plot

Double-octect compounds of non-transition elements with  $AB_2$  formula unit contain oxides and chalcogenides of tetravalent ions (e.g. Si) and halides of divalent ions (e.g. Ca). Moreover, for  $A = \text{Pb}$  or  $\text{Sn}$ , there exist materials with  $A$  acting either as a divalent ( $B = \text{F}, \text{Cl}, \text{Br}, \text{I}$ ) or as a tetravalent ( $B = \text{O}, \text{S}, \text{Se}$ ) cation. Here we consider Pb and Sn as tetravalent ions just as C, Si and Ge, and discuss the dihalides separately. We remark that ditellurides are not stable. The same is true for  $\text{CS}_2$ ,  $\text{CSe}_2$  and  $\text{PbSe}_2$ .

Double octects adopt a variety of structures [20, 21, 22] which can be classified according to different criteria [20], i.e. the coordination number (CN, from 2 to 9), the type of atomic grouping which can be either packed (3d) or layered (2d) or formed by weakly bound molecular units ( $\text{CO}_2$ ). Moreover, a number of them, e.g.  $\text{SiO}_2$ , form good glasses. Therefore, a good structural map must show all these distinctive features.

Figure 1 displays the structural map we obtain with the coordinates introduced in Section I and with the value  $w = 3$  for our parameter in equation (1a). (This appears to give the best sorting-out for  $w \geq 1$ ). In this way, the  $p$ -states have a higher weight in determining the  $Y$  coordinate, which represents the 'size mismatch' between anions and cations and seems to correlate with the ionicity of the compound (see Andreoni et al. in Ref. 10).  $s$ -states, instead, are more relevant in determining the  $X$ -coordinate which seems to be crucial for the sorting-out of these plots, but at the same time is not so easy to interpret. It has previously been suggested (Andreoni et al. in Ref. 10) that it is inversely correlated with the directionality of the bond.

First of all, we recognize a net distinction between 'three dimensional' (3d) and layer (2d) structures. The border is marked by  $\text{Zn}(\text{Cl}_2, \text{Br}_2)$  which in fact are found in both layer and non-layer configurations [22]:

i) Amongst the four different phases of  $\text{ZnCl}_2$ , three adopt '3d' structures ( $\alpha$ -tetragonal,  $\beta$ -monoclinic,  $\delta$ -C19 $\tau$  [23]) with  $\text{CN} = 4$  and one ( $\gamma$ ) has the '2d' tetragonal (red)  $\text{HgI}_2$ -structure, with  $\text{CN} = 4$ . Indeed, also the  $\beta$ -modification shows a tendency to layering.

ii)  $\text{ZnBr}_2$  crystallizes in three forms, i.e. one ( $\beta$ ) with a '3d' tetragonal structure with  $\text{CN} = 4$  (tetrag.  $\text{ZnBr}_2$ ) and two with true layer structures, i.e.  $\text{CdCl}_2$  ( $\alpha$ ) and red- $\text{HgI}_2$  ( $\gamma$ ), both with  $\text{CN} = 6$ .

$\text{ZnI}_2$ , which is also close to the border '2d'/'3d', adopts essentially layer

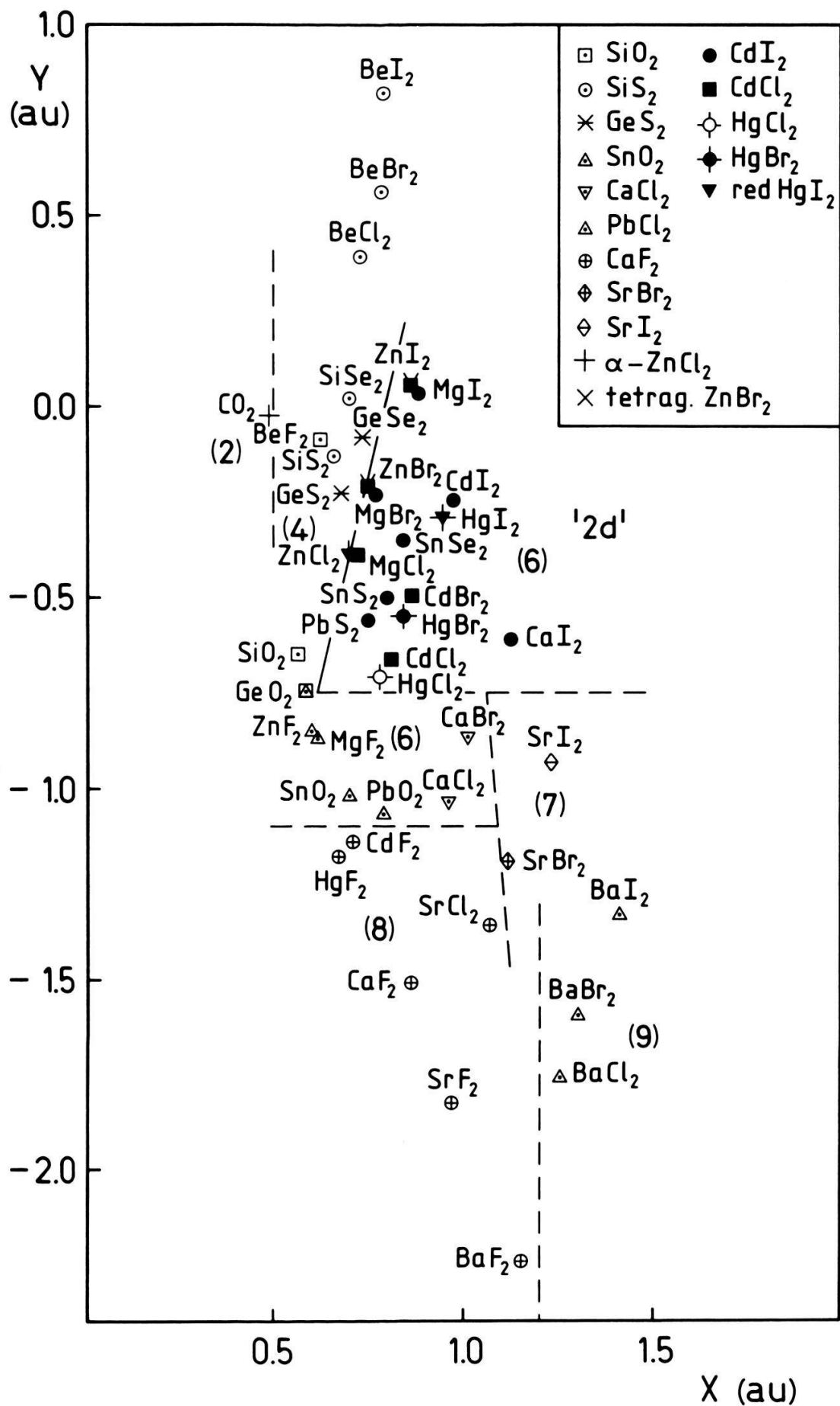


Figure 1  
Structural map of double-octet  $AB_2$  compounds (A = non-transition element) with coordinates defined in the text. Full symbols are used for layer structures. Mixed symbols are used for polymorphic materials, i.e.  $ZnCl_2$ ,  $ZnBr_2$ ,  $ZnI_2$ ,  $HgI_2$ .



structures ( $\text{CdI}_2$ ,  $\text{CdCl}_2$ , red- $\text{HgI}_2$ ) but is also found in the tetragonal  $\text{ZnBr}_2$  configuration.

It is also significant that:

i) Zn-dihalides ( $\text{B} = \text{Cl}, \text{Br}, \text{I}$ ) are located at the border between  $\text{CN} = 4$  and  $\text{CN} = 6$ .

ii)  $\text{GeO}_2$  nicely occurs between the 4-fold structures which we have generally called here of  $\text{SiO}_2$ -type (quartz, cristobalite, tridymite, coesite) and the 6-fold structure named cassiterite [20] ( $\text{SnO}_2$ ) or rutile [21] ( $\text{TiO}_2$ ).

Within the '2d' domain, the  $\text{CdCl}_2$  and  $\text{CdI}_2$  configurations differ in the close-packing of the anions, which is cubic in the former and hexagonal in the latter. The difference is subtle and a few compounds crystallize in both structures depending on the growth mechanism. We do not find a net separation in Fig. 1. Also, we must mention an additional layer modification which is not reported in Fig. 1, for sake of simplicity: the so called  $\text{Cd}(\text{OH})\text{Cl}$  structure which is very close to the  $\text{CdCl}_2$  one (the difference is only in the stacking of the anion layers) and is found for  $\text{CdBr}_2$  and  $\text{CdI}_2$ .

The coordination number (CN) increases with decreasing  $Y$  and/or increasing  $X$ . Separation between structures with different CN's is very well represented in Fig. 1: The unique arrangements adopted by  $\text{SrBr}_2$  and  $\text{SrI}_2$ , and the  $\text{PbCl}_2$ -configuration, for which only average CN's can be defined, also emerge quite clearly in the plot. The more complex  $\text{CN} = 6$  domain is well separated in structures with sheets (2d) and close-packing (3d) of the anions. In the latter,  $\text{CaCl}_2$  corresponds to a slight distortion from the cassiterite [20]. A more important distortion from the cassiterite gives rise to the  $\alpha\text{-PbO}_2$  structure ( $\text{CN} = 6$ ), which is found for  $\text{PbO}_2$  in addition to the more common rutile modification.

The only compounds which are somewhat misplaced in our plot, are mercury dihalides, with the exception of the difluoride found at the correct position. In fact,  $\text{HgCl}_2$  has a unique structure which is layered (as our plot indicates) but, following Hulliger [23], the layers are formed by 'fishbone-like arrays': Thus, it is classified with  $\text{CN} = 2$  by Hulliger. However, the arrangement with sheets of  $\text{HgCl}_2$  molecules is not related at all to the molecular '3d' one of  $\text{CO}_2$  or  $\text{N}_2\text{O}$ .  $\text{HgBr}_2$  possesses an unusual structure which is orthorhombic and layer-like, but the first coordination can be considered as a strongly distorted octahedron. Thus, its occurrence in the plot in the 6-fold and layer domain is still meaningful.  $\text{HgI}_2$  adopts the  $\text{HgBr}_2$  structure at high temperatures (yellow) but is otherwise found in a special layered configuration (red- $\text{HgI}_2$ ), with  $\text{CN} = 4$ . The reason for the misplacement of mercury compounds is not obvious. However, one can reasonably expect that at least the basic approximation involved in the use of nodal (as well as pseudopotential) radii (i.e. the frozen core approximation) loses its validity for heavy and highly polarizable ions like Hg. Also the assumption that only  $s$  and  $p$  states participate in the bond is probably not well founded.

It is interesting to look now at structural changes of the  $\text{AB}_2$  compounds, and see if our plot is consistent with experiment. This is a stringent criterion for the validity of the plot, and a further check of the relative positions of the different domains. In the ionic domain, the general sequence of structural transformations under pressure [24] is rutile  $\xrightarrow{\text{(i)}}$  fluorite  $\xrightarrow{\text{(ii)}}$   $\text{PbCl}_2$  (e.g.  $\text{CdF}_2$  at  $p = 52 \text{ Kb}$ ), which corresponds in the plot to decreasing  $Y$  and increasing  $X$ , respectively.  $\text{ZnF}_2$  at high pressures ( $p > 50 \text{ Kb}$ ) and high temperatures ( $T \approx 1700^\circ\text{C}$ ) adopts

instead the  $\alpha$ - $PbO_2$  structure [21], which also corresponds to a decrease in  $Y$  (see the position of  $PbO_2$  relative to  $ZnF_2$  in Fig. 1). Still in the ionic domain, the sequence of structural transitions driven by temperature increase is  $PbCl_2 \rightarrow$  fluorite (e.g.  $BaCl_2$  at  $920^\circ C$ ) and fluorite  $\rightarrow$  anion-disordered phase (superionic conductor) [25] (with the exception of  $HgF_2$  and  $CdF_2$  which occur here much closer to the 6-fold region than the rest). In the covalent (4-fold) domain, pressure induced transformations do not seem to involve an increase of CN: e.g.  $SiO_2$  adopts the coesite structure, both  $SiS_2$  and  $GeS_2$  transform to  $\alpha$ - $ZnCl_2$  (increase of  $X$  in the plot). The high temperature phases of  $GeS_2$  and  $GeSe_2$  are layered, still with tetrahedral coordination [22].

Especially interesting information comes from the location of glass-forming materials, e.g.  $GeS_2$ ,  $GeSe_2$ ,  $SiO_2$ ,  $SiS_2$ ,  $BeF_2$ ,  $ZnCl_2$ , which occur between the molecular regime (here represented only by  $CO_2$ ) and the layered materials. This is consistent with Phillips' view of glasses [26], as formed by covalent clusters which interact via strong van-der-Waals forces.

Finally, we remark that our 'Y' coordinate for the alkaline-earth dihalides can also be used to classify the corresponding  $AB_2$  molecules. Very recently, it has been pointed out [27] that the occurrence of linear or bent molecules is related to the polarizability of the cation and the ionic radius of the anion. Looking at experimental data (quoted in Ref. 27), we find that all the alkaline-earth dihalide molecules with  $y > y_c \approx -1.25$  au are linear and those with  $y < y_c$  are bent with the apex angle departing from  $180^\circ$  according to the values of ' $y_c - y$ '. This criterion also correctly extends to predict the linearity of the molecules  $ZnF_2$ ,  $HgF_2$  and  $HgCl_2$ .

We find that it is not possible to classify in the same plot (Fig. 1) both the (oxides, chalcogenides) and the dihalides of multivalent cations like Pb and Sn. Let us consider Pb-compounds in detail. With our coordinates,  $PbF_2$  would occur in the fluorite region, which is the room-temperature modification of  $PbF_2$ .  $Pb(Cl_2, Br_2, I_2)$  would all occur in the '2d' region. This would be correct only for  $PbI_2$ , but we consider it fortuitous.  $PbCl_2$  and  $PbBr_2$  both adopt the  $PbCl_2$  structure, just as the dihalides of Ba (well separated in the plot of Fig. 1). The reason why the same coordinates, and in particular  $X$ , cannot be appropriate to describe both chalcogenides and halides is in the type of bonding. In the halides, Pb and Sn ( $Sn(F_2, Cl_2)$ ) behave as divalent ions and the  $s$ -states are not involved directly in the bond. In a steric picture with ionic radii, one would consider different cation radii for the two degrees of ionization and for different CN (e.g. Shannon radii [28] for Pb are  $r(Pb^{2+}) = 1.49$  Å in  $PbCl_2$ ,  $r(Pb^{4+}) = 0.915$  Å in  $PbO_2$ ). Nodal radii (as well as pseudo-potential radii) are defined for each element relative to the rare-gas configuration of the previous row, and have fixed values. It is not surprising that the coordinates of a simple bidimensional plot can still depend on the type of bond.

### III. Comparison with previous work

As mentioned in I, Burdett et al. [10, 13] have presented a couple of years ago a structural map of  $AB_2$  compounds, with A belonging also to the transition series. As coordinates, they chose Zunger's  $R_\sigma$ -coordinates (mismatch average radius) of the two elements,  $X = R_\sigma(B)$ ,  $Y = R_\sigma(A)$  with  $R_\sigma(E) = |S_1(E) - S_0(E)|$ . We report in Fig. 2 Burdett et al.'s plot restricted to the 44 compounds of Fig. 1,

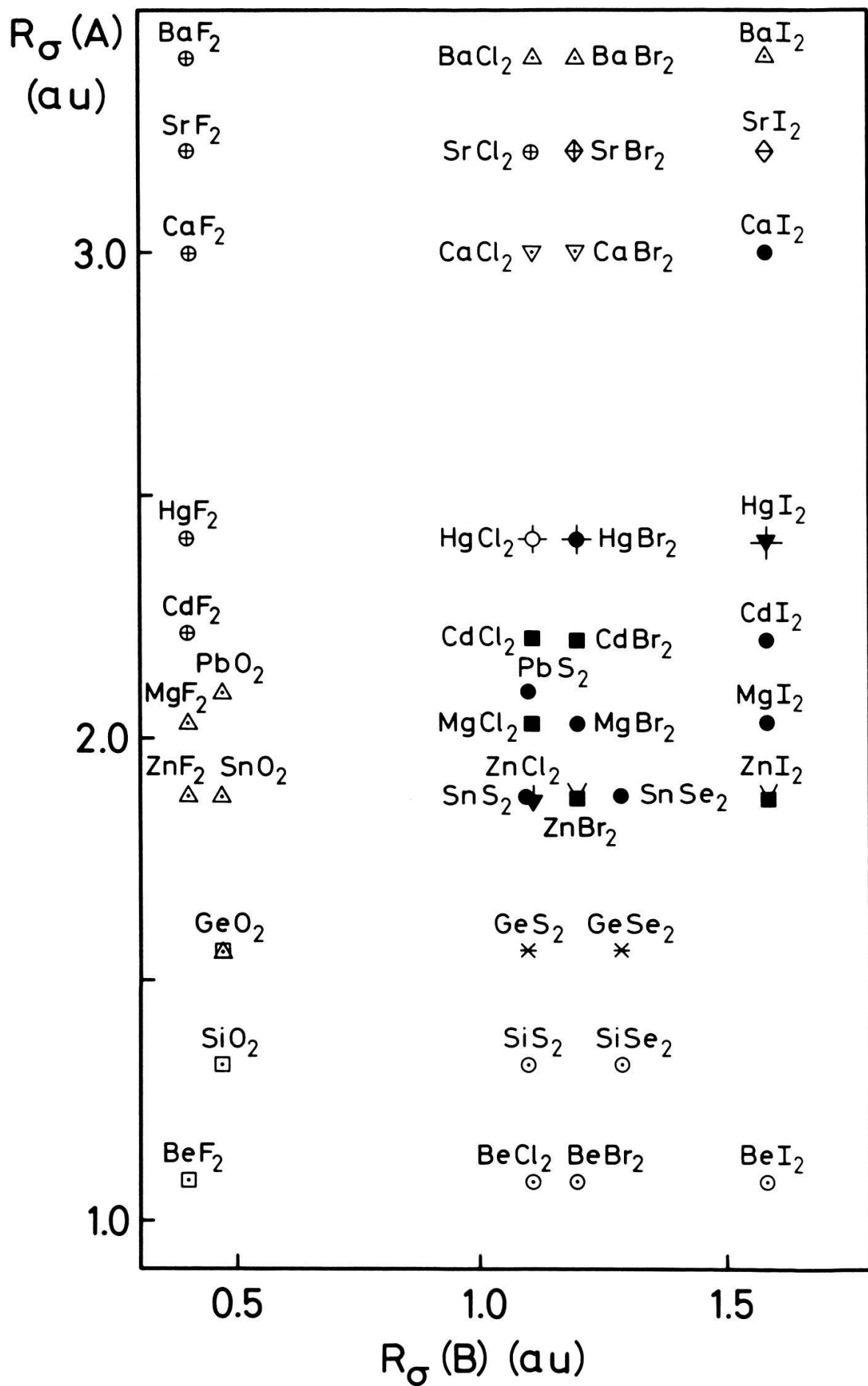


Figure 2  
Structural map of double-octect  $AB_2$  (A = non-transition element) with Burdett et al.'s coordinates (see text). Symbols are defined in the legend of Fig. 1. See also caption of Fig. 1.



and corrected for a more precise assignment of the structures.  $CO_2$  does not appear in the figure but is correctly isolated from the rest since  $R_g(C) = 0.64$ . The difficulties we have found in our scheme are also present in Burdett et al.'s scheme, i.e. Hg-halides are misplaced and Pb/Sn dihalides cannot be included in their plot. (It is easy to see where they would be located in Fig. 2). Moreover, it is sufficient to compare Fig. 2 with Fig. 1, and to go through Section II, to realize that Burdett et al.'s coordinates are much less successful than ours.

## REFERENCES

- [1] See for instance A. R. WILLIAMS and U. VON BARTH, *Theory of the Inhomogeneous Electron Gas*, (eds. S. Lundqvist and N. H. March, Plenum, New York, 1983) pp. 189–308.
- [2] M. T. YIN and M. L. COHEN, Phys. Rev. B 26, 5668 (1983); Phys. Rev. B 29, 6996 (1984) and references therein. P. K. LAM and M. L. COHEN, Phys. Rev. B 24, 4224 (1981). S. G. LOUIE, S. FROYEN and M. L. COHEN, Phys. Rev. B 26, 1738 (1982).
- [3] S. FROYEN and M. L. COHEN, Phys. Rev. B 28, 3258 (1983). S. FROYEN and M. L. COHEN, Phys. Rev. B 27, 3770 (1984).
- [4] M. PARRINELLO, A. RAHMAN and P. VASHISHTA, Phys. Rev. Lett. 50, 1073 (1983).
- [5] M. PARRINELLO and A. RAHMAN, J. Physique C6, 511 (1981).
- [6] V. M. GOLDSCHMIDT, Trans. Faraday Society 25, 253 (1929). L. PAULING, *The Nature of the Chemical Bond and the Structure of Molecules and Crystals*, (Cornell University Press, Ithaca, NY 1960, 3rd edition).
- [7] E. MOOSER and W. B. PEARSON, Acta Cryst. 12, 1015 (1959).
- [8] J. C. PHILLIPS, Rev. Mod. Phys. 42, 317 (1970).
- [9] A. R. MIEDEMA, Philips Tech. Rev. 36, 217 (1976).
- [10] J. ST. JOHN and A. N. BLOCH, Phys. Rev. Lett. 33, 1095 (1974). J. R. CHELIKOWSKY and J. C. PHILLIPS, Phys. Rev. B 17, 2453 (1978). A. ZUNGER and M. L. COHEN, Phys. Rev. B 20, 4082 (1979). W. ANDREONI, A. BALDERESCHI, E. BIÉMONT and J. C. PHILLIPS, Phys. Rev. B 20, 4814 (1979). A. ZUNGER, Phys. Rev. B 22, 5839 (1980). J. K. BURDETT, G. D. PRICE and S. L. PRICE, Phys. Rev. B 24, 2903 (1981).
- [11] J. C. PHILLIPS, Comments Solid State Phys. 9, 11 (1978). A. N. BLOCH and G. SCHATTEMAN, in *Structure and Bonding in Crystals*, (eds. M. O'Keeffe and A. Navrotsky, Academic, New York, 1981) p. 49; A. ZUNGER, ibidem, p. 73. E. MOOSER, Il Nuovo Cimento 2D, 1613 (1983).
- [12] See especially A. ZUNGER in Ref. 10.
- [13] J. K. BURDETT, Acc. Chem. Res. 15, 34 (1982).
- [14] M. NATAPOFF, J. Phys. Chem. Solids 36, 57 (1975); 37, 59 (1976); Chem. Phys. Lett. 78, 375 (1981).
- [15] W. ANDREONI, A. BALDERESCHI and G. GUIZZETTI, (unpublished).
- [16] For a review see: W. KOHN and P. VASHISHTA, *Theory of the Inhomogeneous Electron Gas*, (eds. S. Lundqvist and N. H. March, Plenum, New York, 1983), p. 79. Calculations with different approximations for the correlation energy have been performed in Ref. 15.
- [17] E. CLEMENTI and C. ROETTI, Atomic Data and Nuclear Data Tables, Vol. 14 (1974); A. D. McLEAN and R. S. McLEAN, ibid, vol. 26 (1981).
- [18] F. HERMAN and G. SKILLMAN, *Atomic Structure Calculations*, (Prentice-Hall, Englewood Cliffs, NJ, 1963).
- [19] Calculations were performed with a computer program written by P. Descleaux as a relativistic extension to [18].
- [20] R. W. G. WYCKOFF, *Crystal Structures*, Vol. 1 (Interscience, New York, 1964).
- [21] LANDOLT-BÖRNSTEIN, *Crystal Structure Data of Inorganic Compounds*, Vol. 7 (Springer-Verlag, Berlin-Heidelberg, 1973).
- [22] F. HULLIGER, *Structural Chemistry of Layer-Type Phases*, (ed. F. Lévy) (D. Reidel Publ. Company, Dordrecht, Holland, 1976).
- [23] See Ref. 22 p. 41.
- [24] C. W. F. T. PISTORIUS, Progr. Sol. St. Chem. 11, 1 (1976).
- [25] See for instance C. R. A. CATLOW, Comments Solid State Phys. 9, 157 (1980).
- [26] See especially J. C. PHILLIPS, J. Non-Cryst. Solids 43, 37 (1981).
- [27] G. GALLI and M. P. TOSI, Il Nuovo Cimento B, in press.
- [28] R. D. SHANNON, Acta Cryst. A 32, 751 (1976).